

# Efficient Multi-View Graph Clustering with Local and Global Structure Preservation

Yi Wen\*  
Suyuan Liu\*  
wenyi21@nudt.edu.cn  
suyuanliu@nudt.edu.cn  
National University of Defense  
Technology  
Changsha, China

Ke Liang  
liangke200694@126.com  
National University of Defense  
Technology  
Changsha, China

Xinhang Wan  
wanxinhang@nudt.edu.cn  
National University of Defense  
Technology  
Changsha, China

Xinwang Liu†  
xinwangliu@nudt.edu.cn  
National University of Defense  
Technology  
Changsha, China

Siwei Wang  
wangsiwei13@nudt.edu.cn  
Intelligent Game and Decision Lab  
Beijing, China

Xihong Yang  
Pei Zhang  
xihong\_edu@163.com  
zhangpei@nudt.edu.cn  
National University of Defense  
Technology  
Changsha, China

## ABSTRACT

Anchor-based multi-view graph clustering (AMVGC) has received abundant attention owing to its high efficiency and the capability to capture complementary structural information across multiple views. Intuitively, a high-quality anchor graph plays an essential role in the success of AMVGC. However, the existing AMVGC methods only consider single-structure information, i.e., local or global structure, which provides insufficient information for the learning task. To be specific, the over-scattered global structure leads to learned anchors failing to depict the cluster partition well. In contrast, the local structure with an improper similarity measure results in potentially inaccurate anchor assignment, ultimately leading to sub-optimal clustering performance. To tackle the issue, we propose a novel anchor-based multi-view graph clustering framework termed Efficient Multi-View Graph Clustering with Local and Global Structure Preservation (EMVGC-LG). Specifically, a unified framework with a theoretical guarantee is designed to capture local and global information. Besides, EMVGC-LG jointly optimizes anchor construction and graph learning to enhance the clustering quality. In addition, EMVGC-LG inherits the linear complexity of existing AMVGC methods respecting the sample number, which is time-economical and scales well with the data size. Extensive experiments demonstrate the effectiveness and efficiency of our proposed method.

\*Both authors contributed equally to this research.

†Corresponding author

Permission to make digital or hard copies of all or part of this work for personal or classroom use is granted without fee provided that copies are not made or distributed for profit or commercial advantage and that copies bear this notice and the full citation on the first page. Copyrights for components of this work owned by others than the author(s) must be honored. Abstracting with credit is permitted. To copy otherwise, or to publish, to post on servers or to redistribute to lists, requires prior specific permission and/or a fee. Request permissions from [permissions@acm.org](https://permissions.acm.org).

MM '23, October 29–November 3, 2023, Ottawa, ON, Canada.

© 2023 Copyright held by the owner/author(s). Publication rights licensed to ACM.

ACM ISBN 979-8-4007-0108-5/23/10...\$15.00

<https://doi.org/10.1145/3581783.3611986>

## CCS CONCEPTS

• **Computing methodologies** → **Cluster analysis**; • **Theory of computation** → **Unsupervised learning and clustering**.

## KEYWORDS

multi-view graph clustering; large-scale clustering

### ACM Reference Format:

Yi Wen, Suyuan Liu, Xinhang Wan, Siwei Wang, Ke Liang, Xinwang Liu, Xihong Yang, and Pei Zhang. 2023. Efficient Multi-View Graph Clustering with Local and Global Structure Preservation. In *Proceedings of the 31st ACM International Conference on Multimedia (MM '23)*, October 29–November 3, 2023, Ottawa, ON, Canada. ACM, New York, NY, USA, 10 pages. <https://doi.org/10.1145/3581783.3611986>

## 1 INTRODUCTION

With the advent of the information society, data are usually extracted from multiple sensors in real-world applications [21, 26, 29, 30, 56, 67, 77]. Take the video for example, a clip could be decomposed into the picture, sound records, and text descriptions, which are obtained from a camera, microphone, and producer, respectively [31, 50, 52]. Regarding each modality as a view, how to effectively integrate information from different views has turned out to be an essential task in multi-view scenarios [51, 53, 66]. Multi-view graph clustering (MVGC), as the classical unsupervised multi-view methods [12, 32, 34, 36, 38, 57, 74], which can uncover the intrinsic structure of data pairs, is widely adopted in data mining and knowledge discovery [3, 42, 43]. In general, MVGC methods achieve desirable achievement with two essential processes [78], i.e., view-specific graph construction, and the consensus graph fusion. For instance, Li et al. [23] construct the fused latent representations with structural information fusion from different views in a weighted manner.

Despite abundant MVGC algorithms proposed in recent years, most of them suffer the cubic computational overhead  $O(n^3)$  and quadratic space overhead  $O(n^2)$  due to the full graph construction

and decomposition [16, 59, 61], which hinder their application on large-scale scenarios. As a result, anchor-based multi-view graph clustering (AMVGC), which selects typical anchors to denote the whole data, is proposed to enhance the algorithm's efficiency. For instance, Li et al. [25] propose an innovative anchor-based multi-view clustering method by fusing the local structure and diverse features. Shi et al. [48] generate the indicator matrix by an integrated framework that unifies the anchor graph learning and structure rotation.

Two basic structures, i.e., global and local structures, both play crucial roles in numerous AMVGC studies. As shown in Figure 1 (right), the global structure, which captures the relationship between samples and all anchors, usually has a dense correspondence matrix. Meanwhile, the matrix with local structure is always blocky (with an appropriate permutation) owing to only the relationship between samples and one anchor with high similarity being considered. However, the over-scattered global structure leads to learned anchors failing to depict the cluster partition well, while the local structure with an improper similarity measure results in potentially inaccurate anchor assignment. A natural question is whether combining the two structures leads to a better method [33]. The effectiveness of similar thought is demonstrated by other studies in vision [62] and language [45, 63] tasks. Nonetheless, it is non-trivial to incorporate global and local structures in the MVC field due to the objective equation inconsistency. One pioneer work, [9] merged global and local structures to learn the similarity of the original data on the kernel space in a single view case. However, their high time expenditure and single-view scenario limit the scalability of the method. To the best of our knowledge, no generalized framework with global and local structure preservation has been proposed in the field of AMVGC. Besides, existing anchor selection usually uses a heuristic sampling strategy and is separated from the graph learning phase, resulting in the clustering performance dependent on the quality of anchor initialization. For instance, Kang et al. [19] generate fixed anchors in each view by k-means and average the generated anchor graphs into the fusion graph. Because of the randomness and inflexibility of the k-means and sampling strategy, their clustering performance usually exhibits poor stability.

To tackle these problems, we design a novel anchor-based multi-view graph clustering framework termed Efficient Multi-View Graph Clustering with Local and Global Structure Preservation (EMVGC-LG). Specifically, a unified framework with a theoretical guarantee is designed to capture local and global information. Besides, EMVGC-LG jointly optimizes anchor construction and graph learning to enhance the clustering quality. Moreover, we theoretically prove that the proposed paradigm with a global structure can well approximate the local information. In addition, EMVGC-LG inherits the linear complexity of existing AMVGC methods respecting the sample number, which is time-economical and scales well with the data size. Meanwhile, a two-step iterative and convergent optimization algorithm is designed in this paper. We summarize the contributions of this paper as follows:

- We design an anchor graph learning framework termed Efficient Multi-View Graph Clustering with Local and Global Structure Preservation (EMVGC-LG). With the proven properties, the proposed anchor graph paradigm can not only

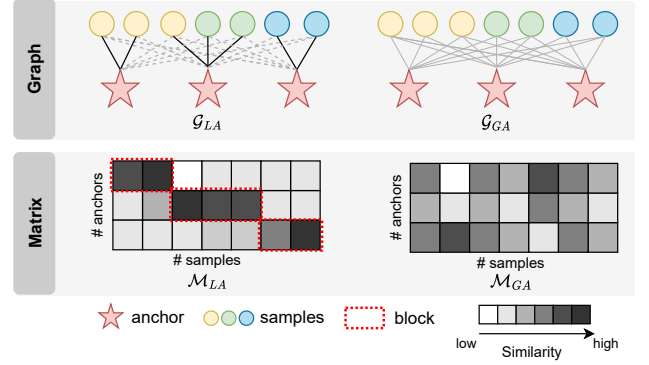


**Figure 1: Two types of the anchor graph: local (left) and global (right). The two types of information often have strong patterns: blocky and dense.  $\mathcal{G}_{LA}$  and  $\mathcal{M}_{LA}$  denote the visualization and matrix of local anchor graph.  $\mathcal{G}_{GA}$  and  $\mathcal{M}_{GA}$  denote the visualization and matrix of global anchor graph.**

capture the global structure between data but also well approximate the local structure.

- In contrast to existing sampling or fixed anchors, the anchor learning and graph fusion processes are jointly optimized in our framework to enhance the clustering quality.
- Extensive experiments on ten benchmark datasets demonstrate the effectiveness and efficiency of our proposed method.

## 2 RELATED WORK

In this section, we present recent research regarding our work, comprising multi-view graph clustering (MVGC) and anchor-based multi-view graph clustering (AMVGC).

### 2.1 Multi-View Graph Clustering

With the given dataset  $\{\mathbf{X}^{(p)}\}_{p=1}^v \in \mathbb{R}^{d_p \times n}$  consisting of  $n$  samples from  $v$  views, the representative multi-view graph clustering (MVGC) model can express as follows:

$$\min_{\mathbf{S}^{(p)}, \mathbf{S}} \sum_{p=1}^v \left\| \mathbf{X}^{(p)} - \mathbf{X}^{(p)} \mathbf{S}^{(p)} \right\|_F^2 + \mu \mathcal{L}(\mathbf{S}^{(p)}, \mathbf{S}),$$

$$\text{s.t.} \begin{cases} \text{diag}(\mathbf{S}^{(p)}) = \mathbf{0}, \mathbf{S}^{(p)\top} \mathbf{1}_n = \mathbf{1}_n, \mathbf{S}^{(p)} \geq \mathbf{0}, \\ \text{diag}(\mathbf{S}) = \mathbf{0}, \mathbf{S}^\top \mathbf{1}_n = \mathbf{1}_n, \mathbf{S} \geq \mathbf{0}, \end{cases}$$

where the first term denotes the data self-representation matrix learning module, and the second term represents the structure integration process performed in  $\{\mathbf{S}^{(p)}\}_{p=1}^v$  to generate a common  $\mathbf{S}$ ,  $\mu$  represents a trade-off parameter,  $\mathcal{L}$  is the regularization term. After obtaining the fused global graph  $\mathbf{S}$ , we need to obtain the spectral embedding  $\mathbf{F} \in \mathbb{R}^{n \times k}$ :

$$\min_{\mathbf{F}} \text{Tr}(\mathbf{F}^\top \mathbf{L} \mathbf{F}), \text{ s.t. } \mathbf{F}^\top \mathbf{F} = \mathbf{I}_k, \quad (1)$$

where  $\mathbf{L}$  denotes the graph Laplace operator, which is calculated by  $\mathbf{D} - \mathbf{W}$ .  $\mathbf{D}$  is a diagonal matrix, and its element is defined as  $d_{ii} = \sum_{j=1}^n s_{ij}$ .  $\mathbf{W}$  is the symmetric similarity matrix, which is

calculated by  $\frac{S+S^T}{2}$ .  $\mathbf{F}$  is the spectral representation [7, 39], and the final clustering label is acquired after the  $k$ -mean algorithm.

Numerous methods have been proposed on the basis of this framework by imposing different constraints [14, 22, 27, 41, 73] or exploring various types of regularization terms [69, 73, 76]. Nie et al. [40] generate the optimal Laplacian matrices by the linear combinations of Laplacian basis matrices constructed from multi-view samples. Gao et al. [4] learn independent representations from each view to capture the diverse information and use a consensus clustering structure to ensure intra-view consistency. Zhang et al. [75] take the view-specific subspace representation as a tensor and explore the intersection information from the diverse views by using low-rank constraints.

Nevertheless, such a paradigm cannot prevent the whole graph construction and consequent spectral decomposition process [17, 60]. The time overhead of the methods is at least  $\mathcal{O}(n^3)$  and the space complexity is at least  $\mathcal{O}(n^2)$ , largely hindering the large-scale applications.

## 2.2 Anchor-based Multi-View Graph Clustering

In recent years, anchor-based multi-view graph clustering (AMVGC) has received abundant attention owing to its high efficiency. By constructing the relationship between the representative anchors selected and samples, i.e., anchor graph  $\mathbf{Z}^{(p)}$ , to recover the full graph, the space complexity of AMVGC can efficiently reduce from  $\mathcal{O}(n^3)$  to  $\mathcal{O}(nm)$  [6, 44].

To our knowledge, a data point within a subspace could be calculated as a linear combination of other data from the same subspace, which is known as the self-expression proposition [15, 47]. Therefore, AMVGC methods can count on the self-expression property for the purpose of constructing a reliable anchor graph, which we also refer to as the global structure since it utilizes the whole data information. The classical anchor-based multi-view graph clustering with global structure can be shown as follows:

$$\begin{aligned} \min_{\mathbf{Z}} \sum_{p=1}^v \left\| \mathbf{X}^{(p)} - \mathbf{A}^{(p)} \mathbf{Z} \right\|_F^2 + \mu \|\mathbf{Z}\|_F^2, \\ \text{s.t. } \mathbf{Z}^T \mathbf{1}_m = \mathbf{1}_n, \mathbf{Z} \geq \mathbf{0}, \end{aligned} \quad (2)$$

where  $\mathbf{A}^{(p)}$  denotes the anchor matrix from the  $p$ -th view, and  $\mathbf{Z}$  denotes the common anchor graph. The final clustering indicates matrix can be calculated from the SVD decomposition of  $\mathbf{Z}$  [19, 64, 65]. Consequently, the computational and space expenditure is reduced from  $\mathcal{O}(n^3)$  to  $\mathcal{O}(vnm)$ , where  $n$ ,  $m$ , and  $v$  denotes the number of samples, anchors, and views, correspondingly.

Based on a specific similarity measure, local structure only considers the relationship between samples and one anchor with high similarity. The significance of preserving local manifold structure has been well recognized in non-linear model and cluster analysis [47, 58] since neighboring samples usually maintain consistent label information. A classical anchor-based multi-view graph clustering with local structure can be calculated by

$$\begin{aligned} \min_{\mathbf{z}} \sum_{p=1}^v \sum_{i=1}^n \sum_{j=1}^m \left\| \mathbf{x}_i^{(p)} - \mathbf{a}_j^{(p)} \right\|_2^2 z_{ji} + \mu_1 \sum_{i=1}^n \sum_{j=1}^m z_{ji}^2, \\ \text{s.t. } \mathbf{z}_i \geq \mathbf{0}, \mathbf{z}_i^T \mathbf{1} = 1, \end{aligned} \quad (3)$$

where  $\mathbf{x}_i^{(p)}$  is the  $i$ -th data from the  $p$ -th view,  $\mathbf{a}_j^{(p)}$  is the  $j$ -th anchor from the  $p$ -th view,  $\mathbf{z}_i$  denotes the  $i$ th column of  $\mathbf{Z}$ , and  $\mu$  is the balance parameter that constrains  $\mathbf{z}_i \geq \mathbf{0}$  and  $\mathbf{z}_i^T \mathbf{1} = 1$  guarantee the probabilistic properties of  $\mathbf{z}_i$ .

## 3 METHOD

### 3.1 Problem Formulation

Intuitively, a high-quality graph plays an important role in the success of graph-based clustering [2, 11, 28, 35, 37, 70–72]. Most multi-view graph clustering (MVGC) methods usually adopt a self-representation strategy to characterize the samples. Although the global structure is well-explored, the local structure is ignored, which provides insufficient information for the learning task and ultimately leads to sub-optimal clustering performance [5, 10, 54]. Several attempts have been made to address the issues [46]. For instance, He et al. [9] merged global and local structures to generate the similarity of the original data in the kernel space. Wen et al. [58] uses low-rank constraints to produce adaptive graphs for the purpose of one-step clustering. However, their high time and space expenditure hinder the application of the method.

In this paper, we employ an anchor strategy, which selects representative samples to capture the manifold structure. Besides, we adopt the view-independent anchor and generate a common anchor graph to efficiently excavate the complementary and consistent information of multiple views. With the view-specific anchor  $\mathbf{A}^{(p)} \in \mathbb{R}^{d_p \times m}$  and the consistent anchor graph  $\mathbf{Z} \in \mathbb{R}^{m \times n}$ , the classical anchor-based multi-view graph clustering with global structure Eq.(2) can be formulated into the following equivalence problem:

$$\begin{aligned} \min_{\mathbf{Z}} \sum_{p=1}^v \text{tr} \left( \mathbf{Z}^T \mathbf{A}^{(p)T} \mathbf{A}^{(p)} \mathbf{Z} \right) - 2 \sum_{p=1}^v \text{tr} \left( \mathbf{X}^{(p)T} \mathbf{A}^{(p)} \mathbf{Z} \right) + \mu \text{tr} \left( \mathbf{Z}^T \mathbf{Z} \right), \\ \text{s.t. } \mathbf{Z} \geq \mathbf{0}, \mathbf{Z}^T \mathbf{1} = \mathbf{1}, \end{aligned} \quad (4)$$

where the  $\mu$  is balanced hyperparameter of regularization term.

For local structure preserving, we summarize the paradigm of the traditional AMVGC with local structure and introduce the terms  $\text{tr}(\mathbf{A}^{(p)} \text{diag}(\mathbf{Z} \mathbf{1}) \mathbf{A}^{(p)T})$ , which can be mathematically derived from numerous methods, including BIMVC[20], MVASM[8], and MGLSMC[13]. With the local term, our objective equation becomes:

$$\begin{aligned} \min_{\mathbf{Z}} \sum_{p=1}^v \text{tr} \left( \mathbf{Z}^T \mathbf{A}^{(p)T} \mathbf{A}^{(p)} \mathbf{Z} \right) - 2 \sum_{p=1}^v \text{tr} \left( \mathbf{X}^{(p)T} \mathbf{A}^{(p)} \mathbf{Z} \right) \\ + \lambda \sum_{p=1}^v \text{tr} \left( \mathbf{A}^{(p)} \text{diag}(\mathbf{Z} \mathbf{1}) \mathbf{A}^{(p)T} \right) + \mu \text{tr} \left( \mathbf{Z}^T \mathbf{Z} \right), \\ \text{s.t. } \mathbf{Z} \geq \mathbf{0}, \mathbf{Z}^T \mathbf{1} = \mathbf{1}, \end{aligned} \quad (5)$$

where  $\mathbf{X}^{(p)} \in \mathbb{R}^{d_p \times n}$  represents the original data with  $d_p$  dimensions in the  $p$ -th view.

Although the local and global structures are preserved, the quality of our model is highly dependent on the anchor initiation. Most existing anchor-based multi-view graph clustering algorithms use heuristic sampling strategies such as K-means to acquire desirable

anchors. However, the anchor construction, as well as the structure learning are separated from each other, which could restrict the clustering capability. Unlike traditional techniques, we learn anchors automatically instead of sampling in this paper. Finally, we can define the optimization for EMVGC-LG as follows:

$$\begin{aligned} \min_{\mathbf{A}^{(p)}, \mathbf{Z}} \sum_{p=1}^v \text{tr} \left( \mathbf{Z}^\top \mathbf{A}^{(p)\top} \mathbf{A}^{(p)} \mathbf{Z} \right) - 2 \sum_{p=1}^v \text{tr} \left( \mathbf{X}^{(p)\top} \mathbf{A}^{(p)} \mathbf{Z} \right) \\ + \lambda \sum_{p=1}^v \text{tr} \left( \mathbf{A}^{(p)} \text{diag}(\mathbf{Z}\mathbf{1}) \mathbf{A}^{(p)\top} \right) + \mu \text{tr}(\mathbf{Z}^\top \mathbf{Z}). \quad (6) \\ \text{s.t. } \mathbf{Z} \geq 0, \mathbf{Z}^\top \mathbf{1} = \mathbf{1} \end{aligned}$$

**PROPOSITION 1.** By setting  $\lambda \in (0, 1]$ ,  $\mu = \lambda\mu_1$ , minimizing Eq. (3) can be approximated by minimizing Eq. (6).

**PROOF.** By adding the item  $\sum_{p=1}^v \text{tr}(\mathbf{X}^{(p)\top} \mathbf{X}^{(p)})$  not related to the optimized variables, Eq. (6) can be transformed into the following equivalence problem:

$$\begin{aligned} \text{Eq. (6)} &\Leftrightarrow \\ &\lambda \sum_{p=1}^v \left( \text{tr} \left( \mathbf{X}^{(p)\top} \mathbf{X}^{(p)} \right) - 2 \text{tr} \left( \mathbf{X}^{(p)\top} \mathbf{A}^{(p)} \mathbf{Z} \right) + \text{tr}(\mathbf{M}^{(p)} \mathbf{Z}) \right) \\ &+ (1 - \lambda) \sum_{p=1}^v \left( \text{tr} \left( \mathbf{Z}^\top \mathbf{A}^{(p)\top} \mathbf{A}^{(p)} \mathbf{Z} \right) - 2 \text{tr} \left( \mathbf{X}^{(p)\top} \mathbf{A}^{(p)} \mathbf{Z} \right) \right. \\ &\left. + \text{tr} \left( \mathbf{X}^{(p)\top} \mathbf{X}^{(p)} \right) \right) + \lambda \sum_{p=1}^v \text{tr} \left( \mathbf{Z}^\top \mathbf{A}^{(p)\top} \mathbf{A}^{(p)} \mathbf{Z} \right) + \mu \text{tr}(\mathbf{Z}^\top \mathbf{Z}) \\ &= \lambda \sum_{p=1}^v \text{tr} \left( \mathbf{Z}^\top \mathbf{A}^{(p)\top} \mathbf{A}^{(p)} \mathbf{Z} \right) + (1 - \lambda) \sum_{p=1}^v \left\| \mathbf{X}^{(p)} - \mathbf{A}^{(p)} \mathbf{Z} \right\|_F^2 \\ &+ \lambda \sum_{p=1}^v \left( \text{tr} \left( \mathbf{X}^{(p)\top} \mathbf{X}^{(p)} \right) - 2 \text{tr} \left( \mathbf{X}^{(p)\top} \mathbf{A}^{(p)} \mathbf{Z} \right) + \text{tr}(\mathbf{M}^{(p)} \mathbf{Z}) \right) \\ &+ \lambda\mu_1 \text{tr}(\mathbf{Z}^\top \mathbf{Z}) \\ &\geq \lambda \sum_{i=1}^n \sum_{j=1}^m \left( \sum_{p=1}^v \left\| \mathbf{x}_i^{(p)} - \mathbf{a}_j^{(p)} \right\|_2^2 z_{ji} + \mu_1 z_{ji}^2 \right) \Leftrightarrow \text{Eq. (3)} \end{aligned}$$

where  $\text{tr}(\mathbf{M}^{(p)} \mathbf{Z}) = \text{tr} \left( \mathbf{A}^{(p)} \text{diag}(\mathbf{Z}\mathbf{1}) \mathbf{A}^{(p)\top} \right)$ ,  $\mathbf{M}_{i,:}^{(p)} = \left[ \mathbf{q}_1^{(p)}, \dots, \mathbf{q}_m^{(p)} \right]$ ,  $\mathbf{q}_j^{(p)} = \mathbf{A}_{:,j}^{(p)\top} \mathbf{A}_{:,j}^{(p)}$ .  $\square$

**REMARK 1.** Proposition 1 illustrates that the proposed Eq.(6) is an upper bound of Eq.(3). Therefore, our model can approximate the local structure by minimizing Eq.(6). The tradeoff between the global and local structure preservation is adjusted by the parameter  $\lambda$ .

### 3.2 Optimization

When all the variables are considered together, the optimization of Eq.(6) becomes a nonconvex problem, and we address it with an alternating optimization algorithm.

---

#### Algorithm 1 Efficient Multi-View Graph Clustering with Local and Global Structure Preservation (EMVGC-LG)

---

**Input:** multi-views dataset  $\{\mathbf{X}^{(p)}\}_{p=1}^v$ , the number of cluster  $k$ .

- 1: Initialize  $\{\mathbf{A}^{(p)}\}_{p=1}^v$ .
- 2: **repeat**
- 3:   Obtain  $\{\mathbf{A}^{(p)}\}_{p=1}^v$  with Eq. (7).
- 4:   Obtain  $\mathbf{Z}$  with Eq. (10).
- 5: **until** converged
- 6: Obtain  $\mathbf{H}$  by performing SVD on  $\mathbf{Z}$

**Output:** Perform k-means on  $\mathbf{H}$  to obtain discrete labels.

---

**3.2.1 Optimization of Anchor Matrices  $\{\mathbf{A}^{(p)}\}_{p=1}^v$ .** When  $\{\mathbf{Z}^{(p)}\}_{p=1}^v$  is fixed, the optimization for  $\{\mathbf{A}^{(p)}\}_{p=1}^v$  can be written as follows:

$$\begin{aligned} \min_{\mathbf{A}^{(p)}} \sum_{p=1}^v \text{tr} \left( \mathbf{A}^{(p)} \mathbf{Z} \mathbf{Z}^\top \mathbf{A}^{(p)\top} \right) - 2 \text{tr} \left( \mathbf{Z} \mathbf{X}^{(p)\top} \mathbf{A}^{(p)} \right) \\ + \lambda \text{tr} \left( \mathbf{A}^{(p)} \text{diag}(\mathbf{Z}\mathbf{1}) \mathbf{A}^{(p)\top} \right). \quad (7) \end{aligned}$$

Considering the optimization of each  $\mathbf{A}_v$  is independent of the corresponding view. Therefore, we can optimize Eq. (7) by solving the problems as follows,

$$\min_{\mathbf{A}^{(p)}} 2\mathbf{A}^{(p)} \mathbf{Z} \mathbf{Z}^\top + 2\lambda \mathbf{A}^{(p)} \text{diag}(\mathbf{Z}\mathbf{1}) - 2\mathbf{X}^{(p)} \mathbf{Z}^\top. \quad (8)$$

Intuitively,  $\mathbf{A}^{(p)}$  can be calculated by:

$$\mathbf{A}^{(p)} = \mathbf{X}^{(p)} \mathbf{Z}^\top \left( \mathbf{Z} \mathbf{Z}^\top + \lambda \text{diag}(\mathbf{Z}\mathbf{1}) \right)^{-1}. \quad (9)$$

**3.2.2 Optimization of Consistent Anchor Graph  $\mathbf{Z}$ .** When  $\{\mathbf{A}^{(p)}\}_{p=1}^v$  is fixed, the optimization for  $\mathbf{Z}$  can be written as follows:

$$\begin{aligned} \min_{\mathbf{Z}} \sum_{p=1}^v \text{tr} \left( \mathbf{Z}^\top \mathbf{A}^{(p)\top} \mathbf{A}^{(p)} \mathbf{Z} \right) + \lambda \sum_{p=1}^v \text{tr}(\mathbf{M}^{(p)} \mathbf{Z}) \\ - 2 \sum_{p=1}^v \text{tr} \left( \mathbf{X}^{(p)\top} \mathbf{A}^{(p)} \mathbf{Z} \right) + \mu \text{tr}(\mathbf{Z}^\top \mathbf{Z}), \quad (10) \\ \text{s.t. } \mathbf{Z} \geq 0, \mathbf{Z}^\top \mathbf{1} = \mathbf{1}, \end{aligned}$$

where  $\mathbf{M}_{i,:}^{(p)} = \left[ \mathbf{q}_1^{(p)}, \dots, \mathbf{q}_m^{(p)} \right]$ ,  $\mathbf{q}_j^{(p)} = \mathbf{A}_{:,j}^{(p)\top} \mathbf{A}_{:,j}^{(p)}$ .

As mentioned earlier, the above optimization process of  $\mathbf{Z}$  can be easily expressed as the below Quadratic Programming (QP) problem,

$$\begin{aligned} \min \frac{1}{2} \mathbf{Z}_{:,i}^\top \mathbf{Q} \mathbf{Z}_{:,i} + \mathbf{f}_i^\top \mathbf{Z}_{:,i}, \quad (11) \\ \text{s.t. } \mathbf{Z}_{:,i}^\top \mathbf{1} = 1, \mathbf{Z}_{:,i} \geq 0, \end{aligned}$$

where  $\mathbf{Q} = \sum_{p=1}^v \mathbf{A}^{(p)\top} \mathbf{A}^{(p)} + \mu \mathbf{I}$ ,  $\mathbf{f}_i = -\sum_{p=1}^v \left( \mathbf{X}_{:,i}^{(p)\top} \mathbf{A}^{(p)} + \frac{\lambda}{2} \mathbf{M}_{i,:}^{(p)} \right)$ .

Because each column of  $\mathbf{Z}$  is a  $m$ -dimensional vector, the time complexity of this sub-problem is  $O(nm^3)$ . The entire optimization process for solving Eq.(6) is summarized in Algorithm 1.

**Table 1: Benchmark datasets**

Datasets	Samples	Views	Clusters
Reuters12	1200	5	6
Flower17	1360	7	17
Mfeat	2000	2	10
VGGFace50	16936	4	50
Caltech256	30607	4	257
YouTubeFace10	38654	4	10
Cifar10	60000	4	9
Cifar100	60000	4	99
YouTubeFace20	63896	4	20
YouTubeFace50	126054	4	50

### 3.3 Discussions

**3.3.1 Convergence.** As the iterations proceed, two variables of the above optimization procedure will be separately addressed. Since each subproblem has reached the global optimum, the value of the EMVGC-LG function will monotonically decrease and finally reach convergence. Moreover, since the lower bound of the objective function can be easily proved to be  $-\sum_{p=1}^v \text{tr}(\mathbf{X}^{(p)\top} \mathbf{X}^{(p)})$  (by Proposition 1), our proposed EMVGC-LG is proven to converge to the local optimum.

**3.3.2 Space Complexity.** In this paper, the primary memory overhead of our approach is the matrix  $\mathbf{Z} \in \mathbb{R}^{m \times n}$  and  $\mathbf{A}^{(p)} \in \mathbb{R}^{d_p \times m}$ . As a result, the space complexity of EMVGC-LG is  $m(n+d)$ , where  $d = \sum_{p=1}^v d_p$ .  $m \ll n$  and  $d \ll n$  are within our settings. Therefore, the space complexity of EMVGC-LG is  $O(n)$ .

**3.3.3 Time Complexity.** The time complexity of EMVGC-LG is composed of two optimization steps, as previously mentioned. The time complexity of updating  $\{\mathbf{A}^{(p)}\}_{p=1}^v$  is  $O((nmd + m^3)v)$ . When analytically obtaining  $\mathbf{Z}$ , it costs  $O(nm^3)$  for all columns. Therefore, the total time cost of the optimization process is  $O(n(mdv + m^3) + m^3v)$ . Consequently, the computational complexity of EMVGC-LG is  $O(n)$ , which is linearly related to the number of data.

## 4 EXPERIMENT

In this section, we perform numerous experiments to assess our proposed EMVGC-LG. Concretely, we discuss the clustering quality on synthetic and real datasets, the evolution of the objective values, the running time, the sensitivity of the parameters, and the ablation study. Our code is accessible on the <https://github.com/wy1019/EMVGC-LG>.

### 4.1 Synthetic Datasets

In order to visualize the different influences of local and global structure, we performed experiments on a synthetic two-view two-dimensional dataset containing 500 samples extracted from five clusters produced by a Gaussian function. From Figure 2, we can observe that incorporating local and global information can effectively enhance the clustering performance. Compared with a singular structure, our strategy improves the performance by 11.85% and 26.08%, respectively, and yields a clearer partition of clusters.

### 4.2 Real-world Datasets

Ten extensively available datasets were used to assess the validity of the proposed algorithms. The information of the datasets are as follows, including Reuters12<sup>1</sup>, Flower17<sup>2</sup>, Mfeat<sup>3</sup>, VGGFace50<sup>4</sup>, Caltech256<sup>5</sup>, YouTubeFace10<sup>7</sup>, Cifar10<sup>6</sup>, Cifar100<sup>6</sup>, YouTubeFace20<sup>7</sup>, and YouTubeFace50<sup>7</sup>. The detailed information is listed in Table 1. Specifically, Reuters12 is a subset of Reuters, which contains 1200 documents described in five languages, including English, France, German, Italian, and Spanish. Flower17 is a flower dataset with 80 images for each class. Mfeat contains 2000 images of hand-written numbers from 0 to 9. Each sample is expressed by six different feature sets, i.e., 216-dimensional FAC, 76-dimensional FOU, 64-dimensional KAR, 6 MORs, 240-dimensional Pix, and 47-dimensional ZER. VGGFace50 is derived from VGGFace. Caltech256 contains 30607 images spanning 257 object categories. Features were extracted from 60,000 tiny color images of 10 categories and 100 categories in four views of Cifar10 and Cifar100 by ResNet18, ResNet50, and DenseNet121. YoutubeFace10, YoutubeFace20, and YoutubeFace50 are face video datasets withdrawn from YouTube.

### 4.3 Compared Methods

Along with our proposed EMVGC-LG, we run ten state-of-the-art multi-view graph clustering methods for comparison, including Multi-view k-means Clustering on Big Data (RMKM) [1], Parameter-free Auto-weighted Multiple Graph Learning (AMGL) [40], Flexible Multi-View Representation Learning for Subspace Clustering (FMR) [23], Partition Level Multi-view Subspace Clustering (PMSC) [18], Binary Multi-View Clustering (BMVC) [79], Large-scale Multi-view Subspace Clustering in Linear Time (LMVSC)[19], Scalable Multiview Subspace Clustering with Unified Anchors (SMVSC) [49], Multi-view clustering: a Scalable and Parameter-free Bipartite Graph Fusion Method (SFMC) [24], Fast Multiview Clustering via Nonnegative and Orthogonal Factorization (FMCNOF)[68], and Fast Parameter-free Multiview Subspace Clustering with Consensus Anchor Guidance (FPMVS-CAG)[55].

For all the aforementioned algorithms, we set their parameters as their recommended range. In the proposed method, we adjusted  $\lambda$  to  $[10^{-3}, 10^{-2}, 10^{-1}, 1]$ ,  $\mu$  to  $[0, 10^{-4}, 1, 10^4]$ , and the anchor numbers to  $[k, 2k, 5k]$ , with a grid search scheme. In addition, we repeated each experiment 10 times to calculate the mean performance and standard deviation. To assess the clustering performance, we use three widely used metrics, consisting of Accuracy (ACC), Normalised Mutual Information (NMI), and Fscore. All experiments were conducted on a desktop computer with Intel core i9-10900X CPU and 64G RAM, MATLAB 2020b (64-bit).

### 4.4 Experimental Results

Table 2 indicates the clustering performance on ten datasets. The best results are marked in red, and the second-best results are

<sup>1</sup><https://archive.ics.uci.edu/ml/datasets/reuters-21578+text+categorization+collection>

<sup>2</sup><https://www.robots.ox.ac.uk/vgg/data/flowers/17/>

<sup>3</sup><http://www.svcl.ucsd.edu/projects/crossmodal/>

<sup>4</sup>[https://www.robots.ox.ac.uk/vgg/data/vgg\\_face/](https://www.robots.ox.ac.uk/vgg/data/vgg_face/)

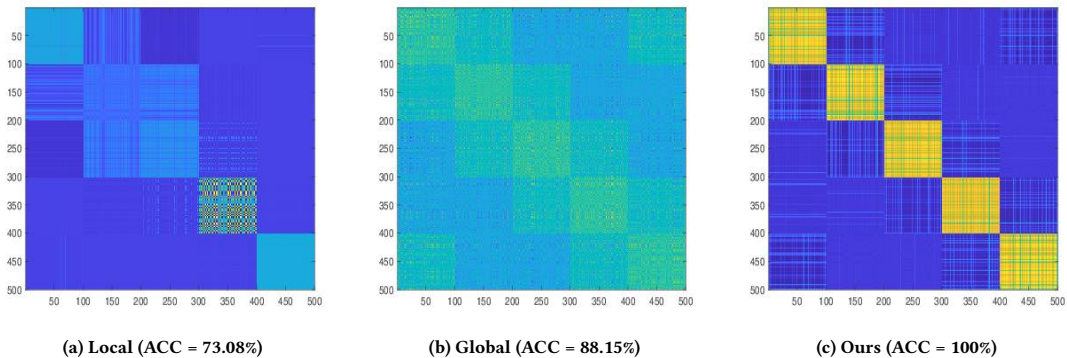
<sup>5</sup><https://authors.library.caltech.edu/7694/>

<sup>6</sup><https://www.cs.toronto.edu/kriz/cifar.html>

<sup>7</sup><https://www.cs.tau.ac.il/wolf/ytfaces/>

**Table 2: Empirical evaluation and comparison of EMVGC-LG with ten baseline methods on ten benchmark datasets**

Dataset	RMKM	AMGL	FMR	PMSC	BMVC	LMVSC	SMVSC	SFMC	FMCNOF	FPMVS-CAG	Proposed
ACC (%)											
Reuters12	44.00±0.00	18.12±0.42	52.35±1.90	27.88±0.75	50.33±0.00	47.92±2.98	<b>55.69±3.06</b>	17.08±0.00	28.58±0.00	45.82±3.29	<b>60.74±2.01</b>
Flower17	23.24±0.00	9.70±1.53	33.43±1.75	20.82±0.74	26.99±0.00	<b>37.12±1.86</b>	27.13±0.84	7.57±0.00	17.43±0.00	25.99±1.83	<b>53.28±2.51</b>
Mfeat	80.80±0.00	71.42±5.42	64.53±2.28	66.41±4.40	65.80±0.00	<b>82.86±6.95</b>	65.57±3.99	56.90±0.00	56.95±0.00	65.11±4.18	<b>88.53±4.87</b>
VGGFace50	8.23±0.00	2.95±0.35	O/M	O/M	10.30±0.00	10.56±0.26	<b>13.36±0.60</b>	3.64±0.00	5.51±0.00	12.06±0.36	<b>15.29±0.74</b>
Caltech256	9.87±0.00	O/M	O/M	O/M	8.63±0.00	9.57±0.17	<b>10.54±0.15</b>	O/M	2.70±0.00	8.78±0.07	<b>11.70±0.36</b>
YouTubeFace10	<b>74.88±0.00</b>	O/M	O/M	O/M	58.58±0.00	74.48±5.30	72.93±3.96	55.80±0.00	43.42±0.00	67.09±5.70	<b>79.55±4.57</b>
CIFAR10	O/M	O/M	O/M	O/M	27.81±0.00	29.02±0.81	<b>29.11±1.35</b>	10.02±0.00	20.53±0.00	26.89±0.71	<b>31.14±1.07</b>
CIFAR100	O/M	O/M	O/M	O/M	8.32±0.00	<b>9.53±0.15</b>	8.34±0.17	1.18±0.00	3.66±0.00	7.29±0.11	<b>10.96±0.35</b>
YouTubeFace20	O/M	O/M	O/M	O/M	57.39±0.00	<b>67.26±3.53</b>	67.13±4.20	O/M	38.61±0.00	63.08±3.79	<b>72.79±2.73</b>
YouTubeFace50	O/M	O/M	O/M	O/M	66.00±0.00	<b>68.32±2.45</b>	O/M	O/M	21.66±0.00	64.24±2.97	<b>70.52±2.62</b>
NMI (%)											
Reuters12	26.83±0.00	3.46±0.76	31.43±0.84	14.76±0.58	27.25±0.00	27.86±1.49	<b>32.46±1.72</b>	12.61±0.00	7.15±0.00	24.59±3.20	<b>35.80±1.03</b>
Flower17	22.07±0.00	10.25±4.01	30.65±0.91	19.13±0.48	25.62±0.00	<b>35.37±1.10</b>	25.78±0.76	7.87±0.00	14.68±0.00	25.81±1.59	<b>51.77±1.72</b>
Mfeat	82.28±0.00	77.12±2.19	66.21±0.73	63.29±1.63	59.39±0.00	<b>82.46±2.79</b>	57.99±2.11	68.15±0.00	55.47±0.00	57.77±2.73	<b>82.90±2.78</b>
VGGFace50	9.66±0.00	2.04±0.50	O/M	O/M	13.48±0.00	12.64±0.28	<b>16.21±0.49</b>	1.63±0.00	4.74±0.00	14.74±0.55	<b>18.71±0.76</b>
Caltech256	31.01±0.00	O/M	O/M	O/M	31.83±0.00	<b>31.96±0.11</b>	28.27±0.24	O/M	1.60±0.00	22.97±0.21	<b>34.78±0.17</b>
YouTubeFace10	<b>78.83±0.00</b>	O/M	O/M	O/M	54.66±0.00	77.74±2.03	78.57±2.80	77.46±0.00	39.15±0.00	76.11±3.06	<b>82.21±2.97</b>
CIFAR10	O/M	O/M	O/M	O/M	<b>17.90±0.00</b>	17.84±0.53	16.00±0.99	0.16±0.00	10.33±0.00	15.45±0.99	<b>18.22±0.66</b>
CIFAR100	O/M	O/M	O/M	O/M	15.05±0.00	<b>15.40±0.18</b>	14.40±0.20	0.53±0.00	7.04±0.00	13.62±0.16	<b>18.42±0.33</b>
YouTubeFace20	O/M	O/M	O/M	O/M	70.65±0.00	76.78±1.34	<b>78.36±2.39</b>	O/M	45.45±0.00	74.30±1.95	<b>80.57±1.60</b>
YouTubeFace50	O/M	O/M	O/M	O/M	81.90±0.00	<b>82.43±0.78</b>	O/M	O/M	43.03±0.00	82.08±1.07	<b>84.17±0.83</b>
Fscore (%)											
Reuters12	32.18±0.00	28.36±0.01	38.62±0.43	27.25±0.41	35.49±0.00	34.80±1.16	<b>39.12±1.10</b>	27.71±0.00	24.11±0.00	34.14±1.23	<b>43.01±1.29</b>
Flower17	14.35±0.00	11.49±0.34	20.09±0.81	12.33±0.36	16.61±0.00	<b>23.99±0.95</b>	17.53±0.21	10.94±0.00	13.93±0.00	17.29±0.39	<b>38.41±1.74</b>
Mfeat	76.64±0.00	65.74±7.46	58.89±1.02	55.68±2.20	50.87±0.00	<b>78.11±5.34</b>	53.09±2.65	45.62±0.00	45.52±0.00	52.50±3.10	<b>80.93±4.85</b>
VGGFace50	3.69±0.00	3.91±0.02	O/M	O/M	5.10±0.00	5.09±0.15	<b>6.35±0.18</b>	4.16±0.00	4.36±0.00	6.10±0.07	<b>7.93±0.41</b>
Caltech256	<b>7.28±0.00</b>	O/M	O/M	O/M	6.25±0.00	6.00±0.28	5.37±0.20	O/M	1.17±0.00	3.22±0.02	<b>8.70±0.69</b>
YouTubeFace10	66.93±0.00	O/M	O/M	O/M	52.53±0.00	<b>68.93±3.19</b>	68.34±5.78	61.25±0.00	32.88±0.00	66.10±5.06	<b>75.38±4.44</b>
CIFAR10	O/M	O/M	O/M	O/M	<b>21.64±0.00</b>	20.34±0.43	19.70±0.55	18.18±0.00	18.48±0.00	20.58±0.34	<b>20.85±0.54</b>
CIFAR100	O/M	O/M	O/M	O/M	<b>4.37±0.00</b>	3.69±0.05	<b>4.47±0.06</b>	1.98±0.00	2.56±0.00	3.78±0.01	<b>4.36±0.15</b>
YouTubeFace20	O/M	O/M	O/M	O/M	49.04±0.00	<b>62.43±2.91</b>	61.68±5.99	O/M	25.84±0.00	57.81±4.00	<b>68.22±3.48</b>
YouTubeFace50	O/M	O/M	O/M	O/M	57.09±0.00	<b>62.49±2.45</b>	O/M	O/M	15.67±0.00	56.89±3.18	<b>63.34±1.78</b>

**Figure 2: Visualization of learned graph on synthetic datasets.**

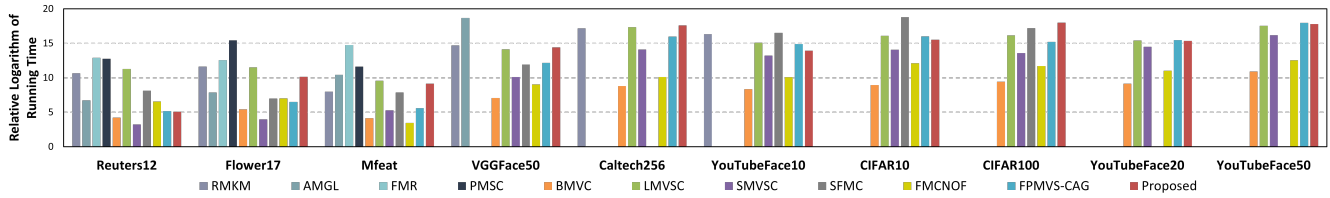


Figure 3: Time comparison of different MVC Methods on ten datasets

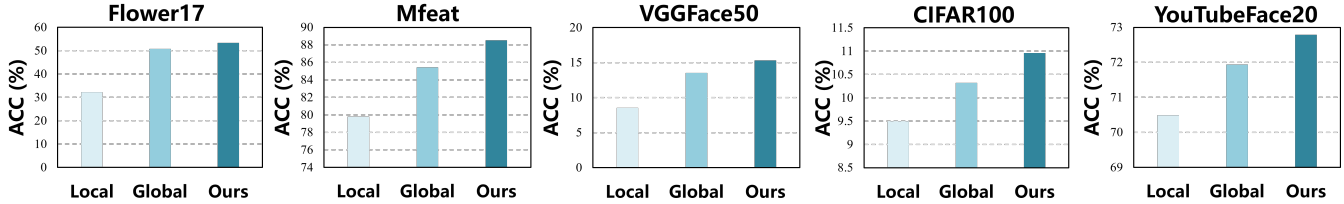


Figure 4: The ablation study of our local and global structure combination strategy on five benchmark datasets.

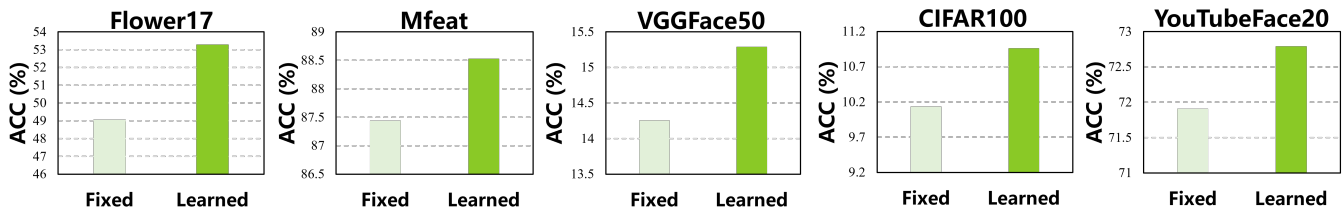


Figure 5: The ablation study of our anchor learning strategy on five benchmark datasets. "Fixed" indicates without our anchor learning strategy.

marked in blue. "O/M" represents the unavailable results due to time-out or out-of-memory errors. According to the results, we have the following observation:

- (1) Compared with existing MVC methods, our proposed algorithm achieves the best or second-best performance on ten datasets. In comparison with the second-best ones, our EMVGC-LG acquires 5.05%, 16.16%, 5.67%, 1.93%, 1.16%, 4.67%, 2.03%, 1.43%, 5.53% and 2.2% in terms of ACC, which demonstrates local and global structure fusion strategy. In other metrics, EMVGC-LG also achieved desirable performance.
- (2) Comparison with classical MVGC methods, i.e., RMKM, AMGL, FMR, and PMSC, encounter scalability problems on large-scale datasets due to the huge matrix computation and memory generated by the full graph construction. Our EMVGC-LG outperforms them by 8.39%, 19.85%, 7.73%, 7.06%, 1.87%, and 4.67% of ACC on six datasets, showing the superiority of our anchor-based algorithm.
- (3) Comparison with existing AMVGC methods, i.e., BMVC, LMVSC, SMVSC, SFMC, FMCNOF, and FPMVS-CAG, our EMVGC-LG still acquires comparable or better performance. In particular, the LMVSC method shows better results than other methods, which demonstrates its superiority in large-scale scenarios. In terms of ACC, our EMVGC-LG achieves better performance

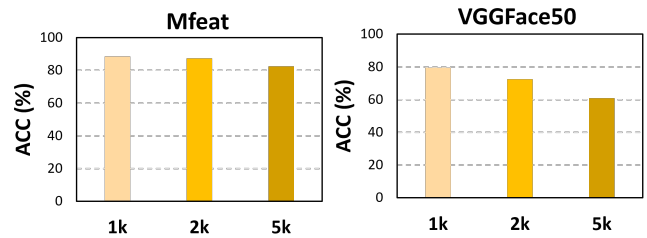


Figure 6: Sensitivity analysis of anchor number  $m$  of our method on two benchmark datasets.

than LMVSC by large margins of 12.82%, 16.16%, 5.67%, 4.73%, 2.13%, 5.07%, 2.12%, 1.43%, 5.53%, and 2.20%, illustrating our effectiveness.

### 4.5 Running Time Comparison

To validate the computational efficiency of the proposed EMVGC-LG, we plot the average running time of each algorithm on ten benchmark datasets in Figure 3. The results of some compared algorithms on large-scale datasets are not reported due to memory

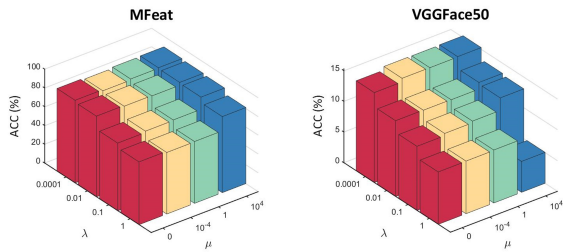


Figure 7: Sensitivity analysis of  $\lambda$  and  $\mu$  of our method on two benchmark datasets.

overflow errors caused by their excessive time and space complexity. As shown in the Figure 3, we can observe that

- (1) Compared to full graph-based clustering methods, the proposed EMVGC-LG significantly reduces run time through the construction of anchor graphs.
- (2) Compared to the anchor-based MVC approach, i.e., SMVSC and FPMVS-CAG, the proposed EMVGC-LG requires more time consumption, mainly due to our local and global structure preservation strategy. Generally, the extra time spent is worthwhile since our proposed EMVGC-LG demonstrates its superiority in most datasets.

## 4.6 Ablation Study

**4.6.1 Local and Global Structure Combination Strategy.** The local and global structure combination strategy is the main contribution of this paper. To further demonstrate the effectiveness of this strategy, we present the experimental results of the ablation study in Figure 4, where "Local" and "Global" indicates only using the local or global structure, respectively. In our experimental setting, we optimize the Eq.(3) and Eq.(2) in the optimization process to obtain the final clustering result. In terms of ACC, the proposed structure combination strategy improves the algorithm performance on the Flower17, Mfeat, VGGFace50, Cifar100, and YouTubeFace20 datasets by **21.03%**, **8.71%**, **6.74%**, **1.46%**, and **2.30%** compared to the simple local structure respectively, which demonstrates the effectiveness of our strategy.

**4.6.2 Anchor Learning Strategy.** We conducted ablation experiments with the proposed anchor learning strategy, as shown in Figure 5. "Fixed" indicates initializing anchors by k-means without updating during the optimization process. Compared to the above methods, our approach significantly improves the clustering performance and avoids the high time expenditure of k-means, demonstrating the effectiveness of the anchor learning strategy.

## 4.7 Convergence and Sensitivity

We conducted several experiments to demonstrate the convergence of the proposed algorithm. As shown in Figure 8, the objective value of our algorithm is monotonically decreasing in each iteration. These results clearly verify the convergence of our proposed algorithm. To investigate the sensitivity of our algorithm to the number of anchors  $m$ , we investigated how our performance shifts for different numbers of anchors. As shown in Figure 6, the number

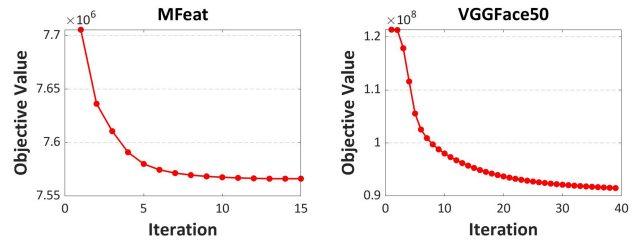


Figure 8: Objective values of the proposed method on two benchmark datasets.

of anchors has some effect on the performance of our algorithm and basically achieves optimal performance at  $m = k$ . Moreover, two hyperparameters,  $\lambda$ , and  $\mu$ , are used in our method,  $\lambda$  is the local and global structure balanced parameter, and  $\mu$  is the coefficient of the sparsity regularization term. As is shown in Figure 7, we conducted comparative experiments on two benchmark datasets to illustrate the impact of these two parameters on performance. In terms of VGGFace50, our method performs better when  $\lambda$  is less than 0.001, and  $\mu$  is larger than 1. When the value of  $\lambda$  is larger than 0.01, EMVGC-LG works well on the Mfeat dataset, and  $\mu$  has little effect on it. Thus, with fixed  $\lambda$ , the variation of  $\mu$  has a smaller effect on the final performance on most datasets, while ACC with the same  $\mu$  will be affected by  $\lambda$ .

## 5 CONCLUSION

In this paper, we propose a novel anchor-based multi-view graph clustering framework termed Efficient Multi-View Graph Clustering with Local and Global Structure Preservation (EMVGC-LG). Specifically, EMVGC-LG considers preserving the local and global structures in a unified framework, which provides comprehensive information for clustering. We theoretically prove that the proposed paradigm with the global structure can well approximate the local information. Besides, anchor construction and graph learning are jointly optimized in our unified framework to enhance the clustering quality. In addition, EMVGC-LG inherits the linear complexity of existing AMVGC methods respecting the sample number, which is time-economical and scales well with the data size. Extensive experiments demonstrate the effectiveness and efficiency of our proposed method. In the future, we will explore the relationship between local and global structure in more detail, e.g., under what circumstances is local structure preferable to global structure?

## 6 ACKNOWLEDGMENTS

This work was supported by the National Key R&D Program of China (no. 2020AAA0107100) and the National Natural Science Foundation of China (project no. 62325604, 62276271).

## REFERENCES

- [1] Xiao Cai, Feiping Nie, and Heng Huang. 2013. Multi-view k-means clustering on big data. In *Twenty-Third International Joint conference on artificial intelligence*.
- [2] Man-Sheng Chen, Ling Huang, Chang-Dong Wang, and Dong Huang. 2020. Multi-view clustering in latent embedding space. In *Proc. of AAAI*.



- [3] Qing Chen, Xiumin Li, Anguo Zhang, and Yongduan Song. 2022. Neuroadaptive Tracking Control of Affine Nonlinear Systems Using Echo State Networks Embedded With Multicentered Structure and Intrinsic Plasticity. *IEEE Transactions on Cybernetics* (2022).
- [4] Hongchang Gao, Feiping Nie, Xuelong Li, and Heng Huang. 2015. Multi-view subspace clustering. In *Proceedings of the IEEE international conference on computer vision*. 4238–4246.
- [5] Quanxue Gao, Wei Xia, Zhizhen Wan, Deyan Xie, and Pu Zhang. 2020. Tensor-SVD based graph learning for multi-view subspace clustering. In *Proceedings of the AAAI Conference on Artificial Intelligence*, Vol. 34. 3930–3937.
- [6] Jun Guo and Jiahui Ye. 2019. Anchors bring ease: An embarrassingly simple approach to partial multi-view clustering. In *Proc. of AAAI*.
- [7] William L Hamilton. 2020. Graph representation learning. *Synthesis Lectures on Artificial Intelligence and Machine Learning* 14, 3 (2020), 1–159.
- [8] Junwei Han, Jinglin Xu, Feiping Nie, and Xuelong Li. 2020. Multi-view K-Means Clustering with Adaptive Sparse Memberships and Weight Allocation. *IEEE Transactions on Knowledge and Data Engineering* (2020).
- [9] Xiaofei He and Partha Niyogi. 2003. Locality preserving projections. *Advances in neural information processing systems* 16 (2003).
- [10] Dong Huang, Chang-Dong Wang, and Jian-Huang Lai. 2022. Fast multi-view clustering via ensembles: Towards scalability, superiority, and simplicity. *arXiv preprint arXiv:2203.11572* (2022).
- [11] Dong Huang, Chang-Dong Wang, Jiansheng Wu, Jian-Huang Lai, and Chee Keong Kwoh. 2019. Ultra-scalable spectral clustering and ensemble clustering. *IEEE Transactions on Knowledge and Data Engineering* (2019).
- [12] Shudong Huang, Zhao Kang, Ivor W Tsang, and Zenglin Xu. 2019. Auto-weighted multi-view clustering via kernelized graph learning. *Pattern Recognition* (2019).
- [13] Tianyu Jiang, Quanxue Gao, and Xinbo Gao. 2021. Multiple graph learning for scalable multi-view clustering. *arXiv preprint arXiv:2106.15382* (2021).
- [14] Jiaqi Jin, Siwei Wang, Zhibin Dong, Xinwang Liu, and En Zhu. 2023. Deep Incomplete Multi-view Clustering with Cross-view Partial Sample and Prototype Alignment. *arXiv preprint arXiv:2303.15689* (2023).
- [15] Zhao Kang, Zipeng Guo, Shudong Huang, Siying Wang, Wenyu Chen, Yuanzhang Su, and Zenglin Xu. 2019. Multiple Partitions Aligned Clustering. In *Proceedings of the Twenty-Eighth International Joint Conference on Artificial Intelligence, IJCAI-19*. International Joint Conferences on Artificial Intelligence Organization, 2701–2707.
- [16] Zhao Kang, Zhiping Lin, Xiaofeng Zhu, and Wenbo Xu. 2021. Structured Graph Learning for Scalable Subspace Clustering: From Single View to Multiview. *IEEE Transactions on Cybernetics* (2021).
- [17] Zhao Kang, Haiqi Pan, Steven CH Hoi, and Zenglin Xu. 2019. Robust graph learning from noisy data. *IEEE transactions on cybernetics* 50, 5 (2019), 1833–1843.
- [18] Zhao Kang, Xinjia Zhao, Chong Peng, Hongyuan Zhu, Joey Tianyi Zhou, Xi Peng, Wenyu Chen, and Zenglin Xu. 2020. Partition level multiview subspace clustering. *Neural Networks* (2020).
- [19] Zhao Kang, Wangtao Zhou, Zhitong Zhao, Junming Shao, Meng Han, and Zenglin Xu. 2020. Large-scale multi-view subspace clustering in linear time. In *Proceedings of the AAAI Conference on Artificial Intelligence*, Vol. 34. 4412–4419.
- [20] Lusi Li and Haibo He. 2020. Bipartite Graph based Multi-view Clustering. *IEEE Transactions on Knowledge and Data Engineering* (2020).
- [21] Liang Li, Siwei Wang, Xinwang Liu, En Zhu, Li Shen, Kenli Li, and Keqin Li. 2022. Local Sample-Weighted Multiple Kernel Clustering With Consensus Discriminative Graph. *IEEE Transactions on Neural Networks and Learning Systems* (2022), 1–14. <https://doi.org/10.1109/TNNLS.2022.3184970>
- [22] Liang Li, Junpu Zhang, Siwei Wang, Xinwang Liu, Kenli Li, and Keqin Li. 2023. Multi-View Bipartite Graph Clustering With Coupled Noisy Feature Filter. *IEEE Transactions on Knowledge and Data Engineering* (2023), 1–13. <https://doi.org/10.1109/TKDE.2023.3268215>
- [23] Ruihuang Li, Changqing Zhang, Qinghua Hu, Pengfei Zhu, and Zheng Wang. 2019. Flexible Multi-View Representation Learning for Subspace Clustering. In *Proc. of IJCAI*.
- [24] Xuelong Li, Han Zhang, Rong Wang, and Feiping Nie. 2020. Multi-view clustering: A scalable and parameter-free bipartite graph fusion method. *IEEE Transactions on Pattern Analysis and Machine Intelligence* (2020).
- [25] Yeqing Li, Feiping Nie, Heng Huang, and Junzhou Huang. 2015. Large-scale multi-view spectral clustering via bipartite graph. In *Twenty-Ninth AAAI Conference on Artificial Intelligence*.
- [26] Yingming Li, Ming Yang, and Zhongfei Zhang. 2018. A survey of multi-view representation learning. *IEEE transactions on knowledge and data engineering* 31, 10 (2018), 1863–1883.
- [27] Zhenglai Li, Chang Tang, Xinwang Liu, Xiao Zheng, Wei Zhang, and En Zhu. 2021. Consensus graph learning for multi-view clustering. *IEEE Transactions on Multimedia* 24 (2021), 2461–2472.
- [28] Zhenglai Li, Chang Tang, Xiao Zheng, Xinwang Liu, Wei Zhang, and En Zhu. 2022. High-order correlation preserved incomplete multi-view subspace clustering. *IEEE Transactions on Image Processing* 31 (2022), 2067–2080.
- [29] Ke Liang, Lingyuan Meng, Meng Liu, Yue Liu, Wenxuan Tu, Siwei Wang, Sihang Zhou, X Liu, and F Sun. 2022. A Survey of Knowledge Graph Reasoning on Graph Types: Static, Dynamic, and Multimodal. (2022).
- [30] Ke Liang, Sihang Zhou, Yue Liu, Lingyuan Meng, Meng Liu, and Xinwang Liu. 2023. Structure Guided Multi-modal Pre-trained Transformer for Knowledge Graph Reasoning. *arXiv preprint arXiv:2307.03591* (2023).
- [31] Meng Liu, Ke Liang, Bin Xiao, Sihang Zhou, Wenxuan Tu, Yue Liu, Xihong Yang, and Xinwang Liu. 2023. Self-supervised temporal graph learning with temporal and structural intensity alignment. *arXiv preprint arXiv:2302.07491* (2023).
- [32] Meng Liu, Yue Liu, Ke Liang, Siwei Wang, Sihang Zhou, and Xinwang Liu. 2023. Deep Temporal Graph Clustering. *arXiv preprint arXiv:2305.10738* (2023).
- [33] Meng Liu, Jiaming Wu, and Yong Liu. 2022. Embedding global and local influences for dynamic graphs. In *Proceedings of the 31st ACM International Conference on Information and Knowledge Management*. 4249–4253.
- [34] Yue Liu, Ke Liang, Jun Xia, Sihang Zhou, Xihong Yang, Xinwang Liu, and Z. Stan Li. 2023. Dink-Net: Neural Clustering on Large Graphs. In *Proc. of ICML*.
- [35] Yue Liu, Wenxuan Tu, Sihang Zhou, Xinwang Liu, Linxuan Song, Xihong Yang, and En Zhu. 2022. Deep Graph Clustering via Dual Correlation Reduction. In *Proceedings of the AAAI Conference on Artificial Intelligence*, Vol. 36. 7603–7611.
- [36] Yue Liu, Jun Xia, Sihang Zhou, Siwei Wang, Xifeng Guo, Xihong Yang, Ke Liang, Wenxuan Tu, Z. Stan Li, and Xinwang Liu. 2022. A Survey of Deep Graph Clustering: Taxonomy, Challenge, and Application. *arXiv preprint arXiv:2211.12875* (2022).
- [37] Yue Liu, Xihong Yang, Sihang Zhou, and Xinwang Liu. 2023. Simple contrastive graph clustering. *IEEE Transactions on Neural Networks and Learning Systems* (2023).
- [38] Yue Liu, Xihong Yang, Sihang Zhou, Xinwang Liu, Zhen Wang, Ke Liang, Wenxuan Tu, Liang Li, Jingcan Duan, and Cancan Chen. 2023. Hard Sample Aware Network for Contrastive Deep Graph Clustering. In *Proc. of AAAI*.
- [39] Andrew Y Ng, Michael I Jordan, and Yair Weiss. 2002. On spectral clustering: Analysis and an algorithm. In *Advances in neural information processing systems*. 849–856.
- [40] Feiping Nie, Jing Li, Xuelong Li, et al. 2016. Parameter-free auto-weighted multiple graph learning: a framework for multiview clustering and semi-supervised classification. In *IJCAI*. 1881–1887.
- [41] Feiping Nie, Xiaoqian Wang, Michael Jordan, and Heng Huang. 2016. The constrained laplacian rank algorithm for graph-based clustering. In *Proceedings of the AAAI conference on artificial intelligence*, Vol. 30.
- [42] Feiping Nie, Zheng Wang, Lai Tian, Rong Wang, and Xuelong Li. 2020. Subspace sparse discriminative feature selection. *IEEE Transactions on Cybernetics* (2020).
- [43] Feiping Nie, Zinan Zeng, Ivor W Tsang, Dong Xu, and Changshui Zhang. 2011. Spectral embedded clustering: A framework for in-sample and out-of-sample spectral clustering. *IEEE Transactions on Neural Networks* 22, 11 (2011), 1796–1808.
- [44] Qiyuan Ou, Siwei Wang, Sihang Zhou, Miaomiao Li, Xifeng Guo, and En Zhu. 2020. Anchor-based multiview subspace clustering with diversity regularization. *IEEE MultiMedia* 27, 4 (2020), 91–101.
- [45] Yifan Peng, Siddharth Dalmia, Ian Lane, and Shinji Watanabe. 2022. Branchformer: Parallel mlp-attention architectures to capture local and global context for speech recognition and understanding. In *International Conference on Machine Learning*. PMLR, 17627–17643.
- [46] Yazhou Ren, Guoji Zhang, Guoxian Yu, and Xuan Li. 2012. Local and global structure preserving based feature selection. *Neurocomputing* 89 (2012), 147–157.
- [47] Zhenwen Ren and Quansen Sun. 2020. Simultaneous global and local graph structure preserving for multiple kernel clustering. *IEEE transactions on neural networks and learning systems* (2020).
- [48] Shaojun Shi, Feiping Nie, Rong Wang, and Xuelong Li. 2021. Fast multi-view clustering via prototype graph. *IEEE Transactions on Knowledge and Data Engineering* (2021).
- [49] Mengjing Sun, Pei Zhang, Siwei Wang, Sihang Zhou, Wenxuan Tu, Xinwang Liu, En Zhu, and Changjian Wang. 2021. Scalable Multi-view Subspace Clustering with Unified Anchors. In *Proceedings of the 29th ACM International Conference on Multimedia*. 3528–3536.
- [50] Xinhang Wan, Jiyuan Liu, Weixuan Liang, Xinwang Liu, Yi Wen, and En Zhu. 2022. Continual Multi-view Clustering. In *Proceedings of the 30th ACM International Conference on Multimedia*. 3676–3684.
- [51] Xinhang Wan, Jiyuan Liu, Xinwang Liu, Siwei Wang, Yi Wen, Tianjiao Wan, Li Shen, and En Zhu. 2023. One-step Multi-view Clustering with Diverse Representation. *arXiv:2306.05437 [cs.LG]*
- [52] Xinhang Wan, Xinwang Liu, Jiyuan Liu, Siwei Wang, Yi Wen, Weixuan Liang, En Zhu, Zhe Liu, and Lu Zhou. 2023. Auto-weighted Multi-view Clustering for Large-scale Data. *arXiv:2303.01983 [cs.LG]*
- [53] Xinhang Wan, Bin Xiao, Xinwang Liu, Jiyuan Liu, Weixuan Liang, and En Zhu. 2023. Fast Continual Multi-View Clustering with Incomplete Views. *arXiv:2306.02389 [cs.LG]*

- [54] Chang-Dong Wang, Jian-Huang Lai, and S Yu Philip. 2015. Multi-view clustering based on belief propagation. *IEEE Transactions on Knowledge and Data Engineering* (2015).
- [55] Siwei Wang, Xinwang Liu, Li Liu, Wenxuan Tu, Xinzhong Zhu, Jiyuan Liu, Sihang Zhou, and En Zhu. 2022. Highly-efficient incomplete large-scale multi-view clustering with consensus bipartite graph. In *Proceedings of the IEEE/CVF Conference on Computer Vision and Pattern Recognition*. 9776–9785.
- [56] Yang Wang. 2021. Survey on deep multi-modal data analytics: Collaboration, rivalry, and fusion. *ACM Transactions on Multimedia Computing, Communications, and Applications (TOMM)* 17, 1s (2021), 1–25.
- [57] Yang Wang, Xuemin Lin, Lin Wu, Wenjie Zhang, Qing Zhang, and Xiaodi Huang. 2015. Robust subspace clustering for multi-view data by exploiting correlation consensus. *IEEE Transactions on Image Processing* (2015).
- [58] Guoqiu Wen, Yonghua Zhu, Linjun Chen, Mengmeng Zhan, and Yangcai Xie. 2021. Global and Local Structure Preservation for Nonlinear High-dimensional Spectral Clustering. *Comput. J.* 64, 7 (2021), 993–1004.
- [59] Jie Wen, Zhihao Wu, Zheng Zhang, Lunke Fei, Bob Zhang, and Yong Xu. 2021. Structural deep incomplete multi-view clustering network. In *Proceedings of the 30th ACM International Conference on Information & Knowledge Management*. 3538–3542.
- [60] Jie Wen, Zheng Zhang, Yong Xu, Bob Zhang, Lunke Fei, and Hong Liu. 2019. Unified embedding alignment with missing views inferring for incomplete multi-view clustering. In *Proc. of AAAI*.
- [61] Jie Wen, Zheng Zhang, Zhao Zhang, Lunke Fei, and Meng Wang. 2020. Generalized incomplete multiview clustering with flexible locality structure diffusion. *IEEE transactions on cybernetics* (2020).
- [62] Haiping Wu, Bin Xiao, Noel Codella, Mengchen Liu, Xiyang Dai, Lu Yuan, and Lei Zhang. 2021. Cvt: Introducing convolutions to vision transformers. In *Proceedings of the IEEE/CVF International Conference on Computer Vision*. 22–31.
- [63] Zhanghao Wu, Zhijian Liu, Ji Lin, Yujun Lin, and Song Han. 2020. Lite transformer with long-short range attention. *arXiv preprint arXiv:2004.11886* (2020).
- [64] Deyan Xie, Xiangdong Zhang, Quanxue Gao, Jiale Han, Song Xiao, and Xinbo Gao. 2019. Multiview clustering by joint latent representation and similarity learning. *IEEE transactions on cybernetics* 50, 11 (2019), 4848–4854.
- [65] Yuan Xie, Bingqian Lin, Yanyun Qu, Cuihua Li, Wensheng Zhang, Lizhuang Ma, Yonggang Wen, and Dacheng Tao. 2020. Joint deep multi-view learning for image clustering. *IEEE Transactions on Knowledge and Data Engineering* (2020).
- [66] Jie Xu, Chao Li, Liang Peng, Yazhou Ren, Xiaoshuang Shi, Heng Tao Shen, and Xiaofeng Zhu. 2023. Adaptive Feature Projection With Distribution Alignment for Deep Incomplete Multi-View Clustering. *IEEE Transactions on Image Processing* 32 (2023), 1354–1366.
- [67] Jie Xu, Huayi Tang, Yazhou Ren, Liang Peng, Xiaofeng Zhu, and Lifang He. 2022. Multi-level feature learning for contrastive multi-view clustering. In *Proceedings of the IEEE/CVF Conference on Computer Vision and Pattern Recognition*. 16051–16060.
- [68] Ben Yang, Xuetao Zhang, Feiping Nie, Fei Wang, Weizhong Yu, and Rong Wang. 2020. Fast multi-view clustering via nonnegative and orthogonal factorization. *IEEE Transactions on Image Processing* 30 (2020), 2575–2586.
- [69] Jufeng Yang, Jie Liang, Kai Wang, Paul L Rosin, and Ming-Hsuan Yang. 2019. Subspace clustering via good neighbors. *IEEE transactions on pattern analysis and machine intelligence* 42, 6 (2019), 1537–1544.
- [70] Xihong Yang, Yue Liu, Sihang Zhou, Xinwang Liu, and En Zhu. 2022. Mixed Graph Contrastive Network for Semi-Supervised Node Classification. *arXiv preprint arXiv:2206.02796* (2022).
- [71] Xihong Yang, Yue Liu, Sihang Zhou, Siwei Wang, Xinwang Liu, and En Zhu. 2022. Contrastive Deep Graph Clustering with Learnable Augmentation. *arXiv preprint arXiv:2212.03559* (2022).
- [72] Xihong Yang, Yue Liu, Sihang Zhou, Siwei Wang, Wenxuan Tu, Qun Zheng, Xinwang Liu, Liming Fang, and En Zhu. 2023. Cluster-guided Contrastive Graph Clustering Network. In *Proceedings of the AAAI conference on artificial intelligence*, Vol. 37. 10834–10842.
- [73] Ming Yin, Shengli Xie, Zongze Wu, Yun Zhang, and Junbin Gao. 2018. Subspace clustering via learning an adaptive low-rank graph. *IEEE Transactions on Image Processing* (2018).
- [74] Changqing Zhang, Huazhu Fu, Qinghua Hu, Xiaochun Cao, Yuan Xie, Dacheng Tao, and Dong Xu. 2018. Generalized latent multi-view subspace clustering. *IEEE transactions on pattern analysis and machine intelligence* (2018).
- [75] Changqing Zhang, Huazhu Fu, Si Liu, Guangcan Liu, and Xiaochun Cao. 2015. Low-rank tensor constrained multiview subspace clustering. In *Proceedings of the IEEE international conference on computer vision*. 1582–1590.
- [76] Changqing Zhang, Qinghua Hu, Huazhu Fu, Pengfei Zhu, and Xiaochun Cao. 2017. Latent multi-view subspace clustering. In *Proc. of CVPR*.
- [77] Junpu Zhang, Liang Li, Siwei Wang, Jiyuan Liu, Yue Liu, Xinwang Liu, and En Zhu. 2022. Multiple Kernel Clustering with Dual Noise Minimization. In *Proceedings of the 30th ACM International Conference on Multimedia (Lisboa, Portugal) (MM '22)*. Association for Computing Machinery, New York, NY, USA, 3440–3450. <https://doi.org/10.1145/3503161.3548334>
- [78] Fei Zhang, Siwei Wang, Jingtao Hu, Zhen Cheng, Xifeng Guo, En Zhu, and Zhiping Cai. 2020. Adaptive Weighted Graph Fusion Incomplete Multi-View Subspace Clustering. *Sensors* (2020).
- [79] Zheng Zhang, Li Liu, Fumin Shen, Heng Tao Shen, and Ling Shao. 2018. Binary multi-view clustering. *IEEE transactions on pattern analysis and machine intelligence* 41, 7 (2018), 1774–1782.